

A novel SVPWM for vehicle Buck–Boost Voltage Inverter

Mr. Vadla Mouneshwara Chary

M.Tech (Power Electronics)
Dhruva Institute and Technology
Nalgonda, Telangana 508252

Mr.V.Balu

Assistant Professor
Dhruva Institute and Technology
Nalgonda, Telangana 508252

Abstract:

This paper proposes a space vector pulse width amplitude modulation (SVPWAM) method for a boost voltage source inverter. For a VSI, the switching loss is reduced when compared to a conventional sinusoidal pulse width modulation (SPWM) method. The output harmonic distortion of SVPWAM is lower than that of the SPWM, by using only one-third of the switching frequency compared to the latter one. As a result, it is feasible to use SVPWAM to make the boost inverter suitable for applications that needs high power density, high efficiency and low cost. The application includes DC power source utilization, power grid, induction heating and electric vehicle motor drive.

I. INTRODUCTION

In recent days the grid tie inverter technology has a vast development. Here the solar power which is a dc is converted to ac for tying with the grid. The inverter is required to inject low harmonic current to, in order to increase the efficiency. For this purpose, the switching frequency of the inverter is designed within a high range from 15 to 20 kHz, resulting in the increase in switching loss in the switching device.

To rectify this problem, different types of soft-switching methods have been proposed in [1]–[3]. A diode rectifier with small DC link capacitor have been proposed in [4], [5], [8]–[12]. various types of modulation techniques have been proposed previously such as optimized pulse-width modulation in [13], improved Space-Vector-PWM control for different optimization targets and applications [14]–[16], and discontinuous PWM (DPWM) [17]. Different switching sequence arrangement can also affect the harmonics, power loss and voltage/current ripples [18]. DPWM has been widely used to reduce

the switching frequency, by selecting only one zero vector in one sector. It results in 50% switching frequency reduction. However, if the same output THD is required, DPWM cannot reduce switching loss compared to SPWM. It will also worsen the device heat transfer because the temperature variation. A double 120 flattop modulation method has been proposed in [6] and [7] to reduce the period of PWM switching to only 1/3 of the whole fundamental period. In addition to that, the method is only specified to a fixed topology, which cannot be applied widely. Fig. 1 shows a typical configuration of the series plug-in electric vehicle (PHEV). The inverter is required to inject lowharmonic current to the motor, in order to reduce the winding loss and core loss. For this purpose, the switching frequency of the inverter is designed within a high range from 15 to 20 kHz, resulting in the switching loss increase in switching device and also the core loss increase in the motor stator. To solve this problem, various soft-switching methods have been proposed [1]–[3]. Active switching rectifier or a diode rectifier with small

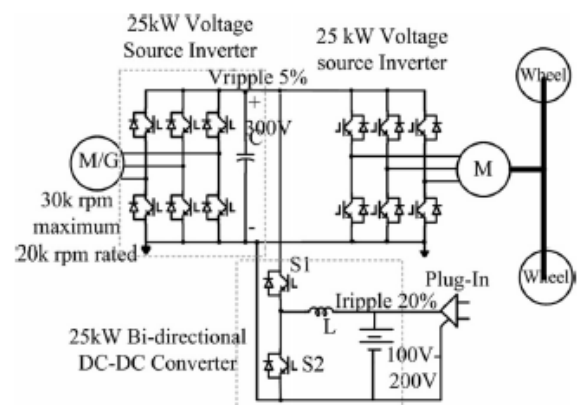


Fig.1. Typical configuration of a series PHEV.

DC link capacitors have been proposed in [4], [5], [8]–[12]. Various types of modulation method have been proposed previously such as optimized pulse-width-modulation [13], improved Space-Vector-PWM control for different optimization targets and applications [14]–[16], and discontinuous PWM (DPWM) [17]. Different switching sequence arrangement can also affect the harmonics, power loss and voltage/current ripples [18]. DPWM has been widely used to reduce the switching frequency, by selecting only one zero vector in one sector. It results in 50% switching frequency reduction. However, if an equal output THD is required, DPWM cannot reduce switching loss than SPWM. Moreover, it will worsen the device heat transfer because of the temperature variation. A double 120 flat-top modulation method has been proposed in [6] and [7] to reduce the period of PWM switching to only 1/3 of the whole fundamental period. However, these papers didn't compare the spectrum of this method with others, which is not fair. In addition, the method is only specified to a fixed topology, which cannot be applied widely.

This paper proposes a novel generalized space vector Pulsewidth amplitude modulation (SVPWAM) method for the buck/boost voltage source inverter (VSI) and current source inverter (CSI). By eliminating the conventional zero vectors in the space vector modulation, two-third and one-third switching frequency reduction can be achieved in VSI and CSI, respectively. If a unity power factor is assumed, an 87% switching loss reduction can be implemented in VSI, and a 74% reduction can be implemented in CSI. A 1-kW boost-converter inverter system has been developed and tested based on the SVPWAM method. A 90% power loss reduction compared to SPWM has been observed. The two stage efficiency reaches 96.7% at the full power rating. The power volume density of the prototype is 2.3 kW/L. The total weight of the system is 1.51 lb. Therefore, a High-efficiency, high-power density, high-temperature, and low-cost 1-kW inverter is achieved by using an SVPWAM method.

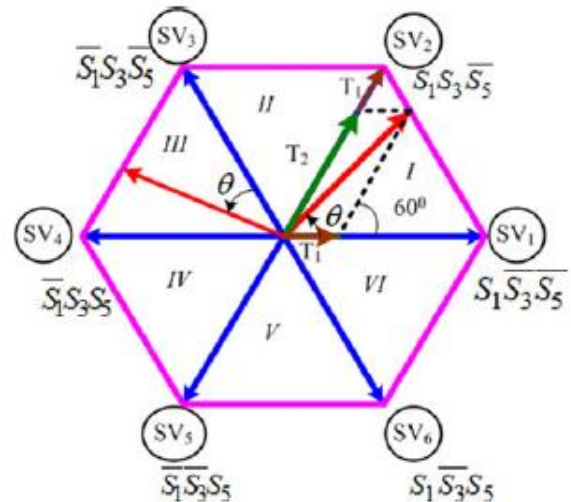


Fig.2. SVPWAM for VSI.

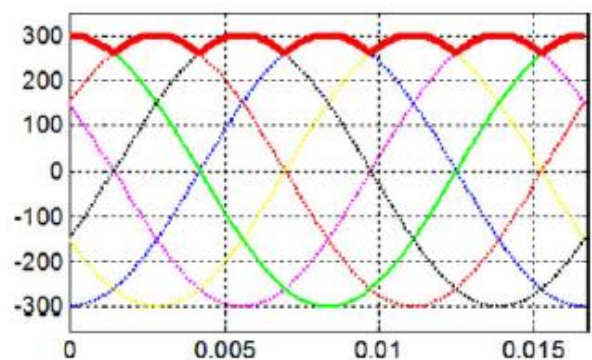


Fig.3. DC-link voltage of SVPWAM in VSI.

2. SVPWAM for VSI

A. Principle of SVPWAM Control in VSI

The principle of an SVPWAM control is to eliminate the zero vectors in each sector. The modulation principle of SVPWAM is shown in Fig.2. In each sector, only one phase leg is doing PWM switching; thus, the switching frequency is reduced by two-third. This imposes zero switching for one phase leg in the adjacent two sectors. For example, in sector VI and I, phase leg A has no switching at all. The dc-link voltage thus is directly generated from the output line-to-line voltage. In sector I, no zero vector is selected. Therefore, S1 and S2 keep constant ON, and S3 and S6 are doing PWM switching. As a result, if the output voltage is kept at the normal three-phase sinusoidal voltage, the dc-link voltage should be equal to line-to-

line voltage V_{ac} at this time. Consequently, the dc-link voltage should present a 6ω varied feature to maintain a desired output voltage. A dc-dc conversion is needed in the front stage to where $\theta \in [0, \pi/3]$ is relative angle from the output voltage vector to the first adjacent basic voltage vector like in Fig. 2. If the time period for each vector maintains the same, the switching frequency will vary with angle, which results in a variable inductor current ripple and multi frequency output harmonics.

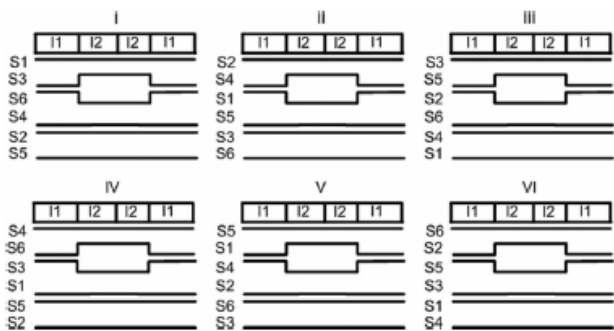


Fig.4. Vector placement in each sector for VSI.

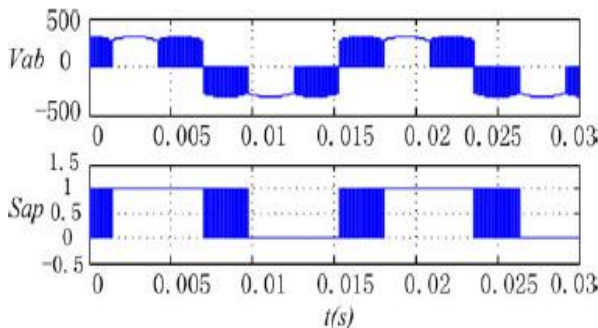


Fig.5. Theoretic waveforms of dc-link voltage, output line-to-line voltage and switching signals.

Where $\theta \in [0, \pi/3]$ is relative angle from the output voltage vector to the first adjacent basic voltage vector like in Fig. 2. If the time period for each vector maintains the same, the switching frequency will vary with angle, which results in a variable inductor current ripple and multi frequency output harmonics. Therefore, in order to keep the switching period constant but still keep the same pulsewidth as the original one, the new time periods can be calculated as

$$T'_1/T_s = T_1/(T_1 + T_2) \quad (2)$$

The vector placement within one switching cycle in each sector is shown in Fig. 4. Fig. 5 shows the output line-to-line voltage and the switching signals of S1.

B. Inverter Switching Loss Reduction for VSI

For unity power factor case, the inverter switching loss is reduced by 86% because the voltage phase for PWM switching is within $[-60^\circ, 60^\circ]$, at which the current is in the zero-crossing region.

In VSI, the device voltage stress is equal to dc-link voltage V_{DC} , and the current stress is equal to output current i_a . Thus the switching loss for each switch is

$$P_{SW_I} = \frac{1}{2\pi} \left[\int_{-\pi/6}^{\pi/6} E_{SR} \frac{|I_m \sin(\omega t)| \cdot V_{DC}}{V_{ref} I_{ref}} \cdot f_{sw} d\omega t + \int_{5\pi/6}^{7\pi/6} E_{SR} \frac{|I_m \sin(\omega t)| \cdot V_{DC}}{V_{ref} I_{ref}} \cdot f_{sw} d\omega t \right] = \frac{2 - \sqrt{3}}{\pi} \cdot \frac{I_m V_{DC}}{V_{ref} I_{ref}} E_{SR} \cdot f_{sw} \quad (3)$$

Where E_{SR} , V_{ref} , I_{ref} are the references.

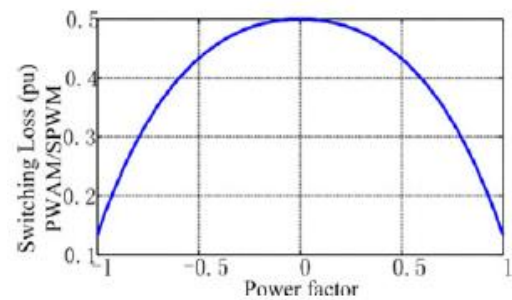


Fig.6. (SVPWM power loss/SPWM power loss) versus power factor in VSI.

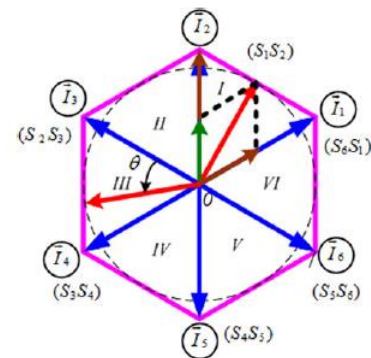


Fig.7. Conventional CSI and its corresponding SVPWM diagram.

Since the SVPWAM only has PWM switching in two 60° sections, the integration over 2π can be narrowed down into integration within two 60°

$$P_{SW_I} = (2\sqrt{3})/\pi \cdot (I_m V_{DC}/(V_{ref} I_{ref})) \cdot E_{SR} \cdot f_{sw} \quad (4)$$

The switching loss for a conventional SPWM method is

$$P_{SW_I'} = (2/\pi) \cdot (I_m V_{DC}/(V_{ref} I_{ref})) \cdot E_{SR} \cdot f_{sw} \quad (5)$$

In result, the switching loss of SVPWAM over SPWM is $f = 13.4\%$.

However, when the power factor decreases, the switching loss reduction amount decreases because the switching current increase as Fig.6 shows.

As indicated, the worst case happens when power factor is equal to zero, where the switching loss reduction still reaches 50%. In conclusion, SVPWAM can bring the switching loss down by 50–87%.

III. SVPWAM FOR CSI

A. Principle of SVPWAM in CSI

The principle of SVPWAM in CSI is also to eliminate the zero vectors. As shown in Fig. 7, for each sector, only two switches are doing PWM switching, since only one switch in upper phase legs and one switch in lower phase legs are conducting together at any moment. Thus, for each switch, it only needs to do PWM

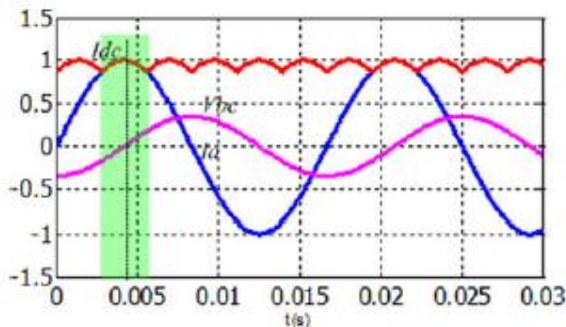


Fig.8. Switching voltage and current when pf = 1.

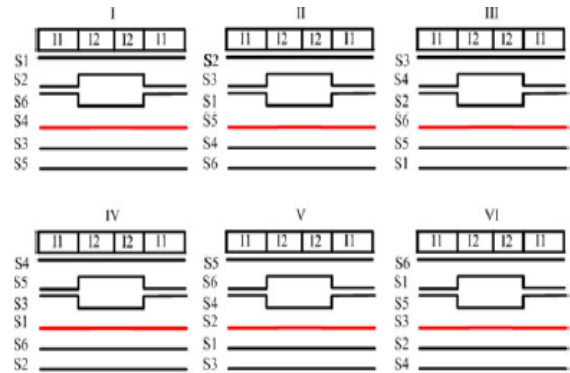


Fig.9. Vector placement for each sector for CSI.

Switching in two sectors, which is one-third of the switching period. Compared to SVPWM with single zero vector selected in each sector, this method brings down the switching frequency by one-third.

Similarly, the dc-link current in this case is a 6ω varied current. It is the maximum envelope of six output currents:

$I_a, I_b, I_c, -I_a, -I_b, -I_c$, as shown in Fig. 8. For example, in sector I, S1 always keeps ON, so the dc-link current is equal to I_a . The difference between dc-link current in CSI and dc-link voltage in VSI is dc-link current in CSI is overlapped with the phase current, but dc-link voltage in VSI is overlapped with the line voltage, not the phase voltage

The time intervals for two adjacent vectors can be calculated in the same way as (1) and (2). According to diagram in Fig. 7, the vector placement in each switching cycle for six switches can be plotted in Fig. 9.

The SVPWAM is implemented on conventional CSI through simulation. Fig. 10 shows the ideal waveforms of the dc current I_{dc} , the output phase ac current and the switching signals of S1. The switching signal has two sections of PWM in positive cycle, but no PWM in negative cycle at all.

B. Inverter Switching Loss Reduction for CSI

In CSI, the current stress on the switch is equal to the dclinkcurrent, and the voltage stress is equal to output line-to-linevoltage, as shown the shadow area in Fig. 8 Thus, the switchingloss for a single switch is determined by

$$P_{SW_CSI} = \frac{2 - \sqrt{3} \cdot i_{dc} \cdot V_{l-peak}}{\pi \cdot V_{ref} I_{ref}} E_{SR} f_{sw} \quad (6)$$

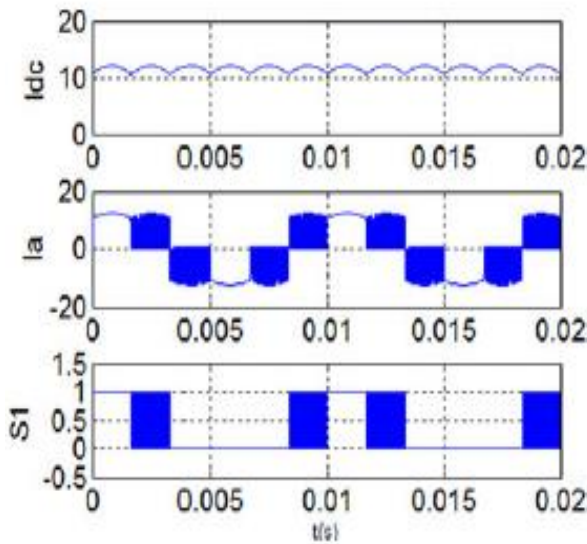


Fig.10. Theoretic waveforms of dc-link current, output line current and switching signals.

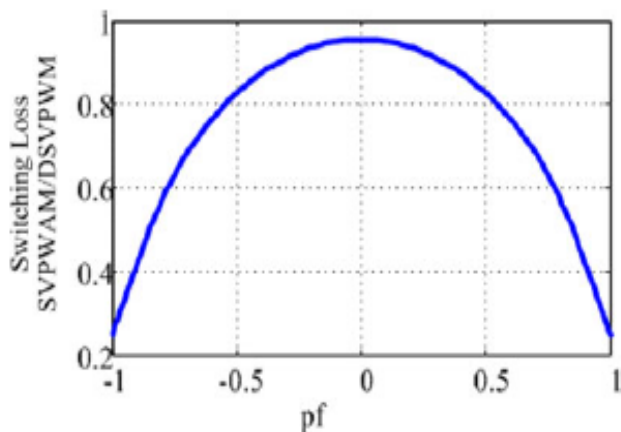


Fig.11.CSI switching loss ratio between SVPWAM and discontinuousSVPWM versus power factor.

When compared to discontinuousSVPWM,if the half switchingfrequency is utilized, then the switching loss of it becomeshalf of the result in (6). The corresponding switching loss ratiobetween SVPWAM and discontinuous SVPWM is shown inFig. 11.

IV. SPECTRUM ANALYSIS OF SVPWAM

A fair comparison in switching loss should be based on anequal output harmonics level. Thus, the switching loss may notbe reduced if the switching frequency needs to be increased inorder to compensate the harmonics. For example, discontinuousSVPWM has to have double switching frequency to achieve thesame THD as continuous PWM. So the switching loss reductionis much smaller than 50%. Therefore, for the newly proposed SVPWAM, a spectrum analysis is conducted to be comparedwith other methods on the basis of an equal average switchingfrequency, which has not been considered in paper [16].

A. Spectrum Comparison Between SVPWAM, SPWM, and SVPWM

The object of spectrum analysis is the output voltage or currentbefore the filter. The reason is that certain orders of harmonicscan be eliminated by sum of switching functions inVSI or subtraction of switching functions in CSI. The comparisonis between SVPWAM, DPWM, and continuous SVPWM in VSI/CSI. The switching frequency selected for each methodis different, because the comparison is built on an equalized

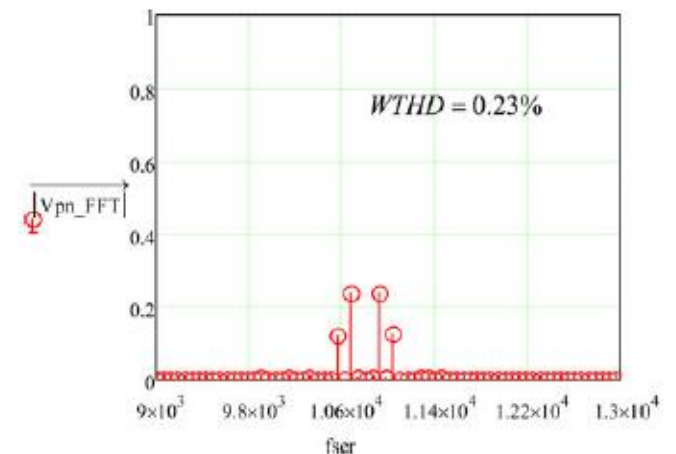


Fig.12. Spectrum of SPWM at switching frequency.

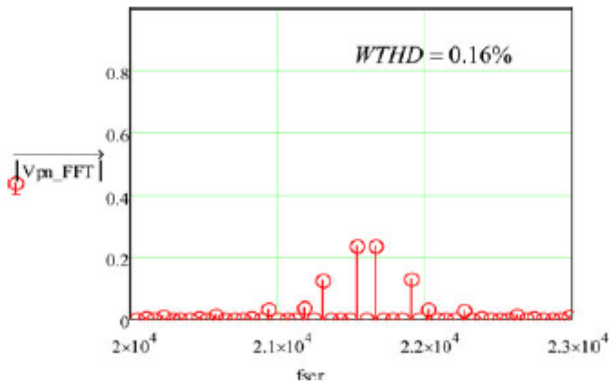


Fig.13. Spectrum of discontinuous SVPWM at switching frequency.

average switching frequency over a whole fundamental cycle, in order to make the harmonics comparable at both low modulation and high modulation range. Assume that the base frequency is $f_0 = 10.8$ kHz. Thus, $3f_0$ should be selected for SVPWM, and f_0 should be selected for continuous SVPWM in VSI. In CSI, $3f_0$, $2f_0$, and f_0 should be selected for SVPWM, discontinuous SVPWM, and continuous SVPWM, respectively.

The modulation index selected here is the maximum modulation index 1.15, since the SVPWM always only has the maximum modulation index. Theoretically, the THD varies with modulation index. The dc-link voltage is designed to be a constant for SVPWM and an ideal 6ω envelope of the output six line-to-line voltages for SVPWM. Thus, the harmonic of the SVPWM here does not contain the harmonics from the dc-dc converter output. It is a direct comparison between two modulation methods from a mathematical point of view.

Figs. 12–14 show the calculated spectrum magnitude at the first side band of switching frequency range for three methods. It can be concluded that the ideal switching function of SVPWM has less or comparable harmonics with SPWM and DPWM.

V. TOPOLOGIES FOR SVPWM

Basically, the topologies that can utilize SVPWM have two stages: dc-dc conversion which converts a dc voltage or current into a 6ω varied dc-link voltage or current; VSI or CSI for which SVPWM is applied. One typical example of this structure is the boost converter inverter discussed previously. However, the same function can also be implemented in a single stage, such as Z/quasi-Z/trans-Z source inverter [37]–[40].

The front stage can also be integrated with inverter to form a single stage. Take current-fed quasi-Z-source inverter as an

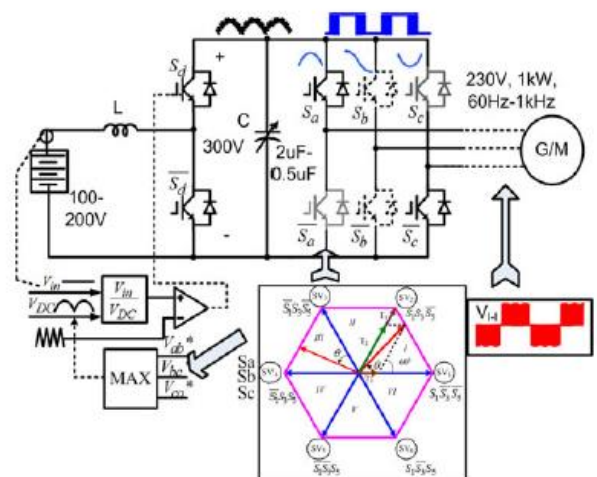


Fig.15. SVPWM-based boost-converter-inverter motor drive system.

Example. Instead of controlling the dc-link current I_{pn} to have a constant average value, the open zero state duty cycle D_{op} will be regulated instantaneously to control I_{pm} to have a 6ω fluctuate average value, resulting in a pulse type 6ω waveform at the real dc-link current I_{pn} , since I_1 is related to the input dc current I_{in} by a transfer function

$$I_1 = \frac{1 - D_{op}}{1 - 2D_{op}} I_{in} \quad (9)$$

VI. CASE STUDY: 1-KWBOOST-CONVERTER INVERTERFOR EV MOTOR DRIVE APPLICATION

A. Basic Control Principle

The circuit schematic and control system for a 1-kW boostconverterinverter motor drive system is shown in Fig. 15. A 6ω dc-link voltage is generated from a constant dc voltage by a boost converter, using open-loop control. Inverter then could be modulated by a SVPWAM method. The specifications for the system are input voltage is 100–200 V; the average dc-link voltage is 300 V; output line-to-line voltage rms is 230 V; and frequency is from 60 Hz to 1 kHz.

B. Voltage Constraint and Operation Region

It is worth noting that the SVPWAM technique can only be applied when the batteries voltage falls into the region $V_{in} \leq \sqrt{3/2} V_l - 1$ due to the step-up nature of boost converter. The constraint is determined by the minimum point of the 6ω dc-link voltage. Beyond this region, conventional SPWM can be implemented. However, the dc-link voltage in this case still varies with 6ω because of the small film capacitor we selected. Thus, a modified SPWM with varying dc-link voltage will be adopted during the motor start up as shown in Fig. 16. Hence, the system will achieve optimum efficiency when the motor is operating a little below or around nominal voltage. When the motor demands a low voltage during start up, efficiency is the same as the conventional SPWM-controlled inverter.

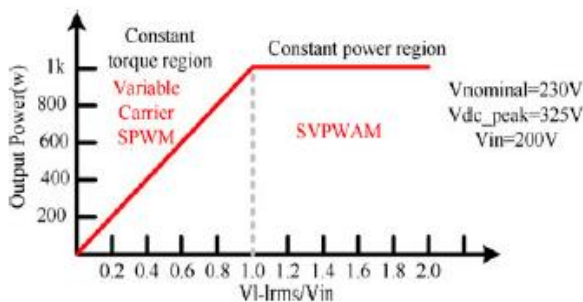


Fig.16. Operation region of boost-converter-inverter EV traction drive.

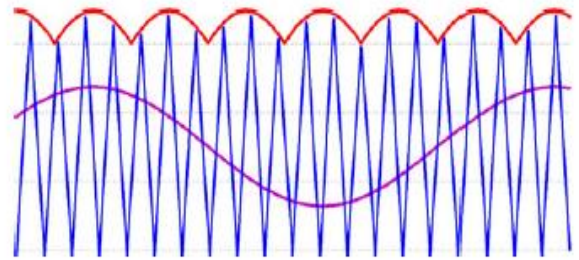


Fig.17. Variable carrier SPWM control in buck mode.

In SVPWAM control of boost mode, dc-link voltage varies with the output voltage, in which the modulation index is always kept maximum. So, when dc-link voltage is above the battery voltage, dc-link voltage level varies with the output voltage. The voltage utilization increased and the total power stress on the devices has been reduced.

C. Variable DC-Link SPWM Control at High Frequency

When the output needs to operate at a relative high frequency, like between 120 Hz and 1 kHz, it is challenging to obtain a 6ω dc-link voltage without increasing the switching frequency of a boost converter. Because the controller does not have enough bandwidth.

Furthermore, increasing boost converter switching frequency would cause a substantial increase of the total switching loss, because it takes up more than 75% of the total switching loss. The reason is because it switches at a complete current region. Also a normal SPWM cannot be used in this range because the capacitor is designed to be small that it cannot hold a constant dc link voltage. Therefore, the optimum option is to control the dc link voltage to be 6ω and do a variable dc link SPWM modulation, as explained in Fig. 17.

In this variable dc-link SPWM control, in order to get better utilization of the dc-link voltage, an integer times between the dc-link fundamental frequency and output frequency is preferred. When the output frequency is in [60 Hz, 120 Hz], a 6ω dc link is chosen; when the frequency is in [120 Hz, 240 Hz], a

3ω dc link is chosen; when the frequency is in [240 Hz, 360 Hz], a 2ω dc link is chosen.

D. Experiment Results

1) Experiment Setup: A 1-kW boost-converter inverter prototype has been built in the laboratory to implement the SVPWAM control at 60 Hz and SPWM control at 1 kHz, in

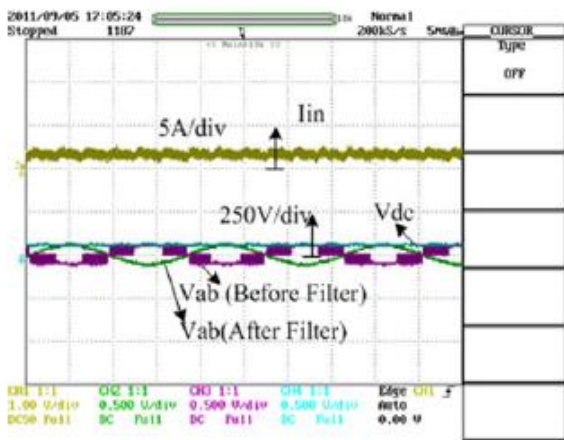


Fig.19. Output voltage and input current at $V_{in} = 20$ V, V_{dc} avg = 60 V, $V_{lrms} = 46$ V, $P_o = 40$ W, $f_o = 60$ Hz, $f_{sw} = 20$ kHz.

order to demonstrate their merits in reducing power loss and reducing the size compared to traditional methods. The picture of the hardware is shown in Fig. 18. It includes a DSP board, a gate drive board, a boost converter, a three-phase inverter, heat sink, and a fan cooling system. The dimension is 11 cm × 8 cm × 5 cm, and the total weight is 1.5 lb.

The parameters used in the test are rated power: 1 kW; battery voltage: 100–200 V; rated line voltage rms: 230 V; dc-link voltage peak: 324 V; switching frequency: 20 kHz; output frequency: 60 Hz–1 kHz

2) SVPWAM Control at 60 Hz: Figs. 19–20 show the output and input voltage, current waveform when input voltage increases from 20 to 100 V, while keeping the boost ratio constant. In this case, the output voltage increases linearly with input voltage increase. The

output power increases in proportion to square of the input voltage.

Fig. 21 shows the efficiency test results by YOKOGAWA WT1600 series power meter when the input voltage increases from 100 to 200 V, while keeping the output power constant at 1 kW. The output line-to-line voltage rms keeps at 230 V, and the dc-link voltage is a 6ω varied waveform with 325 V peak value. In the data record on the power meter, Umn6, Umn4, and Umn1 represent the phase line voltages; Irms6, Irms4, and Irms1 represent ten times of phase currents, because ten circles of wires have been wound on the current transducer core of

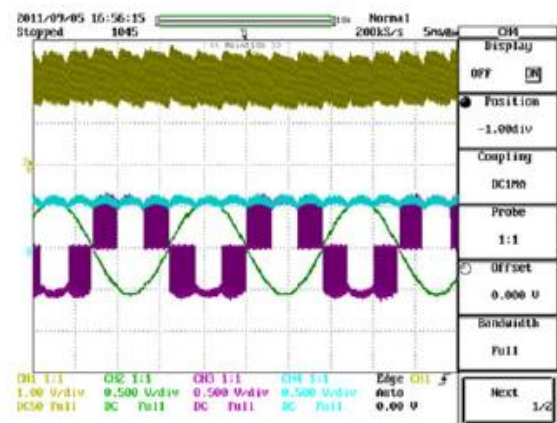
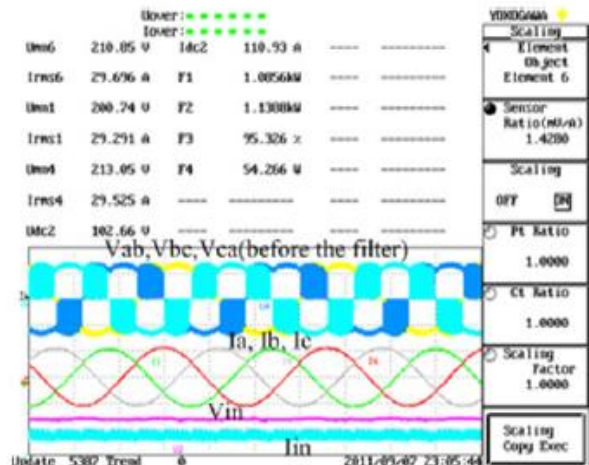


Fig.20. Output voltage and input current at $V_{in} = 100$ V, V_{dc} avg = 300 V, $V_{lrms} = 230$ V, $P_o = 1$ kW, $f_o = 60$ Hz, $f_{sw} = 20$ kHz.



(a)

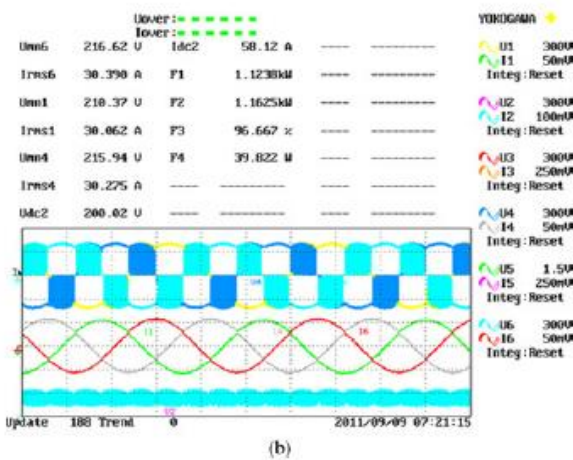


Fig. 21. Results of efficiency test at constant full power rating 1 kW but different input voltage by YOKOGAWA WT1600 series power meter.

Waveforms from the top to bottom: output line-to-line voltage before LC filter, output current, input voltage, input current. The numbers displayed on the screen represent: Umn6, Umn1, Umn4 : RMS value of output line-to-line voltage before LC filter, like the first waveform shows; Irms6, Irms1, Irms4 : ten times of output line current; Udc2 : input voltage; Idc2 : 10 times of input current; F1: output power; F2: input power; F3: efficiency calculated from F1/F2; F4: total power loss: (a) $V_{in} = 150\text{ V}$, $V_{dc\text{ avg}} = 300\text{ V}$, $V_{l\text{ rms}} = 230\text{ V}$, $P_o = 1\text{ kW}$, $f_o = 60\text{ Hz}$, $f_{sw} = 20\text{ kHz}$; (b) $V_{in} = 200\text{ V}$, $V_{dc\text{ avg}} = 300\text{ V}$, $V_{l\text{ rms}} = 230\text{ V}$, $P_o = 1\text{ kW}$, $f_o = 60\text{ Hz}$, $f_{sw} = 20\text{ kHz}$.

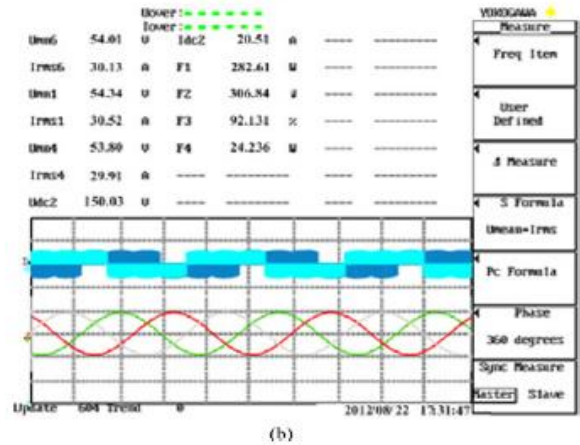


Fig. 22. Results of efficiency test at constant torque region by YOKOGAWA WT1600 series power meter.

Waveforms from the top to bottom: output line-to-line voltage before LC filter, output current. The input voltage keeps at 200 V constant; the dc-link voltage keeps at 300 V 60 voltage; the output voltage changes from 54 to 162 V, thus the power also changes from 280 to 850 W proportionally. When power is equal to 1 kW, the voltage reaches at Nominal value 230 V. (a) $V_{in} = 200\text{ V}$, $V_{dc\text{ avg}} = 300\text{ V}$, $V_{l\text{ rms}} = 162\text{ V}$, $P_o = 850\text{ W}$, $f_o = 60\text{ Hz}$. (b) $V_{in} = 200\text{ V}$, $V_{dc\text{ avg}} = 300\text{ V}$, $V_{l\text{ rms}} = 54\text{ V}$, $P_o = 280\text{ W}$, $f_o = 60\text{ Hz}$.

The power meter. Udc2 is input dc voltage and Idc2 is ten times of average input dc current. F1 and F2 are the measured output and input power, respectively. F3 is the efficiency that is calculated using F1/F2. F4 is the overall power loss. Fig. 22 shows the efficiency test results when the power increases in proportional to output voltage below the maximum power while keeping the input voltage and dc-link voltage constant, which is corresponding to the constant torque region in Fig. 16. The input voltage keeps at 300 V 60 voltages; the output voltage changes from 54 to 162 V; thus, the power also changes from 280 to 850 W proportionally. When power is equal to 1 kW, the voltage reaches at nominal value 230 V; this waveform is shown in Fig. 21(b).

3) Output Three-Phase Voltage at 1 kHz: When the output

Frequency increases to 1 kHz, the measured voltage and current waveforms and efficiency are shown in Fig. 23 at input voltage

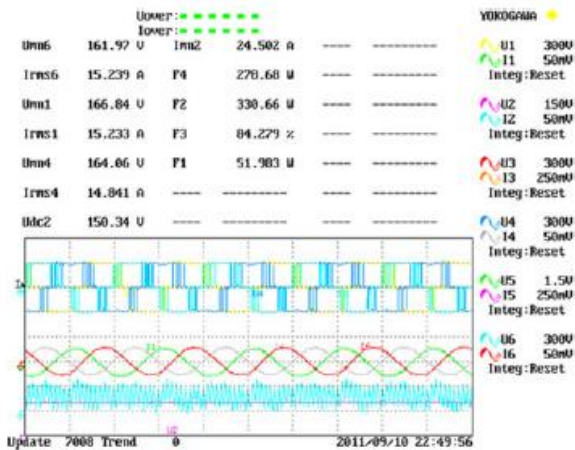


Fig.23. the efficiency test at $V_{in} = 150\text{ V}$ at $f_o = 1\text{ kHz}$: from top to bottom: output line voltage, output current, and input current.

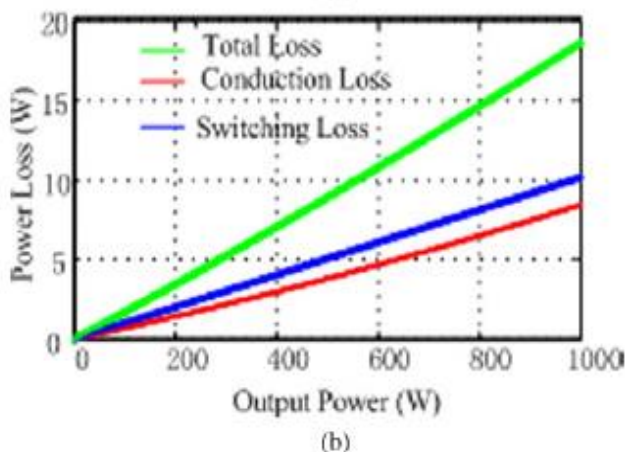
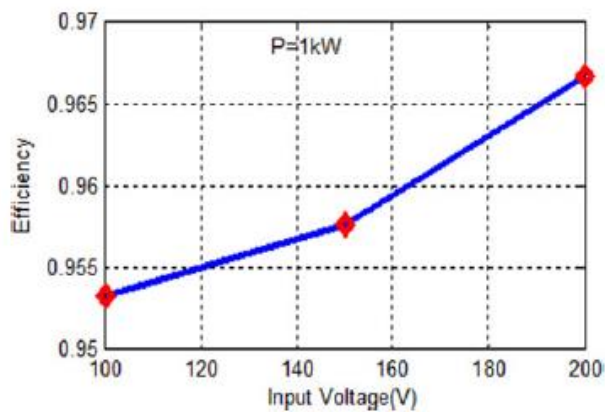


Fig. 26. Comparison between inverter power losses in the condition that d_{link} voltage changes from 0 to full rating at 300 V: (a) SVPWAM, (b) SPWM.

Increases from 0 to full rating under two methods. Since the research target is only inverter, the test condition is based on varying the output power by changing output voltage from 0 to 230 V. It is observed that in the SVPWAM method, conduction loss accounts for 80% of the total power loss, but in the SPWM method, switching loss is higher than conduction loss. The switching loss is reduced from 10 to 1.4 W from SPWM to SVPWAM. An estimated 87% switching loss reduction has been achieved.

VII. CONCLUSION

The SVPWAM control method preserves the following advantages compared to traditional SPWM and SVPWM method.

- 1) The switching power loss is reduced by 90% compared with the conventional SPWM inverter system.
- 2) The power density is increased by a factor of 2 because of reduced dc capacitor (from 40 to 6 μF) and small heatsink is needed.
- 3) The cost is reduced by 30% because of reduced passives, heat sink, and semiconductor stress.

A high-efficiency, high-power density, high-temperature, and low-cost 1-kW inverter engine drive system has been developed and tested. The effectiveness of the proposed method in reduction of power losses has been validated by the experimental results that were obtained from the laboratory scale prototype.

REFERENCES

- [1] D. M. Divan and G. Skibinski, "Zero-switching-loss inverters for high power applications," IEEE Trans. Ind. Appl., vol. 25, no. 4, pp. 634–643, Jul./Aug. 1989.

- [2] W. McMurray, "Resonant snubber with auxiliary switches," *IEEE Trans. Ind. Appl.*, vol. 29, no. 2, pp. 355–362, Mar./Apr. 1993.
- [3] J.-S. Lai, R. W. Young, Sr., G. W. Ott, Jr., J. W. McKeever, and F. Z. Peng, "A delta-configured auxiliary resonant snubber inverter," *IEEE Trans. Ind. Appl.*, vol. 32, no. 3, pp. 518–525, May/Jun. 1996.
- [4] J. S. Kim and S. K. Sul, "New control scheme for ac-dc-ac converter without dc link electrolytic capacitor," in *Proc. 24th Annu. IEEE Power Electron. Spec. Conf.*, Jun. 1993, pp. 300–306.
- [5] K. Rigbers, S. Thomas, U. Boke, and R. W. De Doncker, "Behavior and loss modeling of a three-phase resonant pole inverter operating with 120° double flat top modulation," in *Proc. 41st IAS Annu. Meeting IEEE Ind. Appl. Conf.*, Oct. 8–12, 2006, vol. 4, pp. 1694–1701.
- [6] J. Shen, K. Rigbers, C. P. Dick, and R. W. De Doncker, "A dynamic boost converter input stage for a double 120° flat top modulation based three-phase inverter," in *Proc. IEEE Ind. Appl. Soc. Annu. Meeting*, Oct. 5–9, 2008, pp. 1–7.
- [7] H. Fujita, "A three-phase voltage-source solar power conditioner using a single-phase PWM control method," in *Proc. IEEE Energy Convers. Congr. Expo.*, 2009, pp. 3748–3754.
- [8] H. Haga, K. Nishiya, S. Kondo, and K. Ohishi, "High power factor control of electrolytic capacitor less current-fed single-phase to three-phase power converter," in *Proc. Int. Power Electron. Conf.*, Jun. 21–24, 2010, pp. 443–448.
- [9] X. Chen and M. Kazerani, "Space vector modulation control of an ac-dc-ac converter with a front-end diode rectifier and reduced dc-link capacitor," *IEEE Trans. Power Electron.*, vol. 21, no. 5, pp. 1470–1478, Sep. 2006.
- [10] M. Hinkkanen and J. Luomi, "Induction motor drives equipped with diode rectifier and small dc-link capacitance," *IEEE Trans. Ind. Electron.*, vol. 55, no. 1, pp. 312–320, Jan. 2008.
- [11] J. Jung, S. Lim, and K. Nam, "A feedback linearizing control scheme for a PWM converter-inverter having a very small dc-link capacitor," *IEEE Trans. Ind. Appl.*, vol. 35, no. 5, pp. 1124–1131, Sep./Oct. 1999.
- [12] L. Malesani, L. Rossetto, P. Tenti, and P. Tomasin, "AC/DC/AC PWM converter with reduced energy storage in the dc link," *IEEE Trans. Ind. Appl.*, vol. 31, no. 2, pp. 287–292, Mar./Apr. 1995.
- [13] T. Bruckner and D. G. Holmes, "Optimal pulse-width modulation for three-level inverters," *IEEE Trans. Power Electron.*, vol. 20, no. 1, pp. 82–89, Jan. 2005.
- [14] F. Blaabjerg, S. Freysson, H.-H. Hansen, and S. Hansen, "A new optimized space-vector modulation strategy for a component-minimized voltage source inverter," *IEEE Trans. Power Electron.*, vol. 12, no. 4, pp. 704–714, Jul. 1997.
- [15] M. M. Bech, F. Blaabjerg, and J. K. Pedersen, "Random modulation techniques with fixed switching frequency for three-phase power converters," *IEEE Trans. Power Electron.*, vol. 15, no. 4, pp. 753–761, Jul. 2000.
- [16] F. Blaabjerg, D. O. Neacsu, and J. K. Pedersen, "Adaptive SVM to compensated dc-link voltage ripple for four-switch three-phase voltage-source inverters," *IEEE Trans. Power Electron.*, vol. 14, no. 4, pp. 743–752, Jul. 1999.
- [17] L. Asiminoaei, P. Rodriguez, and F. Blaabjerg, "Application of discontinuous PWM modulation in active power filters," *IEEE Trans. Power Electron.*, vol. 23, no. 4, pp. 1692–1706, Jul. 2008.

[18] B. P. McGrath, D. G. Holmes, and T. Lipo, "Optimized space vectorswitching sequences for multilevel inverters," IEEE Trans. Power Electron.,vol. 18, no. 6, pp. 1293–1301, Nov. 2003.

[19] R. Zhang, V. H. Prasad, D. Boroyevich, and F. C. Lee, "Three-dimensionalspace vector modulation for four-leg voltage-source converters," IEEETrans. Power Electron., vol. 17, no. 3, pp. 314–326, May 2002.

[20] R. Burgos, R. Lai, Y. Pei, F. Wang, D. Boroyevich, and J. Pou, "Spacevector modulator for vienna-type rectifiersbased on the equivalencebetweentwo- and three-level converters: A carrier-based implementation,"IEEE Trans. Power Electron., vol. 23, no. 4, pp. 1888–1898, Jul. 2008.

[21] P. C. Loh, D. M. Vilathgamuwa, Y. S. Lai, G. T. Chua, and Y. Li, "Pulsewidthmodulation of Z-source inverters," IEEE Trans. Power Electron.,vol. 20, no. 6, pp. 1346–1355, Nov. 2005.

[22] F. Z. Peng, "Z-source inverter," IEEE Trans. Ind. Appl., vol. 39, no. 2,pp. 504–510, Mar./Apr. 2003.



Mr.V.BALU he received M.E (Power Systems) from University College of Engineering, Osmania University, Hyderabad in 2008 A.P. Graduated from JNTU University, Hyderabad in the year 2002. Presently he is working as Associate Professor in Dhruva Institute of Engineering & Technology, Hyderabad in the Department of Electrical & Electronics Engineering. He had total 9 years of experience in teaching. His fields of interest include power quality and Power Systems Optimization.



Mr. VADLA MOUNESHWARA CHARY . He is pursuing M.Tech (Power Electronics) at Dhruva Institute of Engineering and Technology. Completed his B.Tech (EEE) from KG Reddy college of engineering and technology. TS